

# 9. GEOCHEMICAL EXPRESSION OF EARLY DIAGENESIS IN MIDDLE EOCENE-LOWER OLIGOCENE PELAGIC SEDIMENTS IN THE SOUTHERN LABRADOR SEA, SITE 647, ODP LEG 105<sup>1</sup>

M. A. Arthur,<sup>2</sup> W. E. Dean,<sup>3</sup> J. C. Zachos,<sup>2</sup> M. Kaminski,<sup>4</sup> S. Hagerty Rieg,<sup>2</sup> and K. Elmsstrom<sup>2</sup>

## ABSTRACT

Geochemical analyses of the middle Eocene through lower Oligocene lithologic Unit IIIC (260–518 meters below seafloor [mbsf]) indicate a relatively constant geochemical composition of the detrital fraction throughout this depositional interval at Ocean Drilling Program (ODP) Site 647 in the southern Labrador Sea. The main variability occurs in redox-sensitive elements (e.g., iron, manganese, and phosphorus), which may be related to early diagenetic mobility in anaerobic pore waters during bacterial decomposition of organic matter. Initial preservation of organic matter was mediated by high sedimentation rates (36 m/m.y.). High iron (Fe) and manganese (Mn) contents are associated with carbonate concretions of siderite, manganosiderite, and rhodochrosite. These concretions probably formed in response to elevated pore-water alkalinity and total dissolved carbon dioxide (CO<sub>2</sub>) concentrations resulting from bacterial sulfate reduction, as indicated by nodule stable-isotope compositions and pore-water geochemistry. These nodules differ from those found in upper Cenozoic hemipelagic sequences in that they are not associated with methanogenesis. Phosphate minerals (carbonate-fluorapatite) precipitated in some intervals, probably as the result of desorption of phosphorus from iron and manganese during reduction.

The bulk chemical composition of the sediments differs little from that of North Atlantic Quaternary abyssal red clays, but may contain a minor hydrothermal component. The silicon/aluminum (Si/Al) ratio, however, is high and variable and probably reflects original variations in biogenic opal, much of which is now altered to smectite and/or opal CT. An increase in the sodium/potassium (Na/K) ratio in the upper Eocene corresponds to the beginning of coarser-grained feldspar flux to the site, possibly marking the onset of more vigorous deep currents.

Although the Site 647 cores provide a nearly complete high-resolution, high-latitude Eocene-Oligocene record, the high sedimentation rate and somewhat unusual diagenetic conditions have led to variable alteration of benthic foraminifers and fine-fraction carbonate and have overprinted the original stable-isotope records. Planktonic foraminifers are less altered, but on the whole, there is little chance of sorting out the nature and timing of environmental change on the basis of our stable-isotope analyses.

## INTRODUCTION

A total of 117 samples of predominantly grayish-green, middle Eocene through lower Oligocene, nannofossil claystone and clayey nannofossil chalk from lithologic Unit IIIC (260–518 mbsf; Cores 105-647A-28R through -54R) in Hole 647A were collected for inorganic geochemical and stable isotopic analyses. The samples were collected initially for the following purposes:

1. To document possible changes in the geochemical composition of sediments and stable isotopic compositions of calcareous biogenic components in response to changes in paleoclimatic and ocean circulation during the late Eocene to early Oligocene at high northern latitudes.

2. To document the composition of unusual authigenic nodules and/or beds in lithologic Unit IIIC.

The generally good core recovery, an apparently complete Eocene/Oligocene transition, and seemingly good (visual) preservation of calcareous microfossils led us to believe that our results would have a bearing on interpretation of climate and circulation

events that occurred in latest Eocene to earliest Oligocene time. However, as shown below, the most significant application for our geochemical and isotopic data is in the documentation of a rather unusual early diagenetic regime.

## METHODS

Samples were freeze-dried and ground to pass through a 100-mesh (149  $\mu\text{m}$ ) sieve. Splits of all samples were analyzed coulometrically (Huffman, 1985) for carbonate and total carbon (precision better than 1%) at the University of Rhode Island (URI). In addition, splits of many samples were sieved and selected for planktonic and benthic foraminifers for stable isotope studies. Splits of the ground samples were analyzed at the U.S. Geological Survey (USGS), Denver, for 10 major and minor elements by X-ray fluorescence (XRF) and 30 major, minor, and trace elements by induction-coupled, argon-plasma emission spectrometry (ICP) (Baedecker, 1987). Nine elements (aluminum, iron, magnesium, calcium, sodium, potassium, titanium, phosphorus, and manganese) were analyzed by both XRF and ICP, with essentially identical results between the two methods. Five samples contained concentrations of iron (Fe) and manganese (Mn) that were sufficiently high to cause interferences with XRF; hence, no XRF results are available for these samples. Analytical results are given in Table 1 and plotted vs. depth in Figures 1 through 6. The geochemical data have not been corrected for contribution of pore-water salts because porosities are typically lower than 40%. Sodium (Na) and magnesium (Mg) concentrations would be the main elements affected.

Carbonate components were analyzed for carbon and oxygen-isotopic compositions at URI. Samples were ground to < 50  $\mu\text{m}$ , roasted *in vacuo* at 390°C for 1 hr and reacted online in purified phosphoric acid at 50°C. The resulting CO<sub>2</sub> gas was purified and introduced into a VG Micromass 602D mass spectrometer for analysis. Results are expressed in the standard delta notation relative to the PDB standard, where

$$\delta = (\text{Rsamp}/\text{Rstd}) \times 1000 \text{ Rstd},$$

and analytical precision was 0.1% for  $\delta^{18}\text{O}$  and 0.05% for  $\delta^{13}\text{C}$ .

<sup>1</sup> Srivastava, S. P., Arthur, M., Clement, B., et al., 1989. *Proc. ODP, Sci. Results*, 105: College Station, TX (Ocean Drilling Program).

<sup>2</sup> Graduate School of Oceanography, University of Rhode Island, Narragansett, RI 02882.

<sup>3</sup> U.S. Geological Survey, Box 25046, MS 939, Federal Center, Denver, CO 80225.

<sup>4</sup> Woods Hole Oceanographic Institution, Woods Hole, MA 02543. Now at Centre for Marine Geology, Dalhousie University, Halifax, Nova Scotia B3H, Canada.

443087	44.00	3.00	87.00	418.36	38.20	10.60	11.15	4.02	3.72	1.56	1.56	21.80	19.60	1.24	1.20	1.67	1.92
444116	44.00	4.00	116.00	420.16	33.50	9.33	10.01	3.43	3.43	1.31	1.36	25.60	23.80	1.03	1.11	1.33	1.80
445074	44.00	5.00	74.00	421.24	29.10	8.06	8.69	3.00	2.86	1.17	1.16	29.90	28.00	0.97	1.04	0.72	1.44
446064	44.00	6.00	64.00	422.64	33.90	9.23	10.01	3.52	3.58	1.34	1.36	25.40	23.80	1.06	1.13	1.06	1.44
451102	45.00	1.00	102.00	425.11	39.80	10.20	10.96	4.39	4.29	1.55	1.56	20.50	19.60	1.15	1.24	1.56	1.68
453055	45.00	3.00	55.00	427.65	38.50	9.63	10.39	4.04	4.00	1.45	1.46	22.30	21.00	0.96	1.12	1.28	1.68
461047	46.00	1.00	47.00	434.27	47.70	11.10	11.71	5.35	5.29	1.76	1.83	14.00	13.30	1.27	1.35	1.59	1.68
462041	46.00	2.00	41.00	435.71	42.70	10.20	10.96	4.26	4.29	1.57	1.64	19.10	18.20	1.28	1.35	1.44	1.56
463041	46.00	3.00	41.00	437.21	46.40	11.50	11.90	5.61	5.29	1.78	1.83	13.80	13.16	1.36	1.32	1.68	1.80
464041	46.00	4.00	41.00	438.71	52.40	13.00	13.60	5.40	5.01	1.95	1.99	9.94	9.52	1.42	1.48	1.85	1.92
465057	46.00	5.00	57.00	440.37	47.00	11.80	12.28	6.48	6.01	1.89	1.83	13.30	12.74	1.31	1.48	1.74	1.92
465111	46.00	5.00	111.00	440.91	29.40	7.52	8.31	3.46	3.29	1.27	1.26	28.10	26.60	1.40	1.62	0.91	1.12
466057	46.00	6.00	57.00	441.87	46.50	11.70	12.28	5.29	5.15	1.76	1.83	14.20	13.30	1.37	1.35	1.65	1.80
471033	47.00	1.00	33.00	443.82	46.70	11.20	11.90	7.27	7.29	1.88	1.99	13.10	12.46	1.30	1.35	1.98	2.16
473016	47.00	3.00	16.00	446.66	49.00	12.50	13.03	5.30	5.15	1.88	1.83	12.20	11.48	1.32	1.35	1.75	1.80
474021	47.00	4.00	21.00	448.21	45.00	11.20	11.90	7.16	7.01	1.85	1.83	13.70	13.02	1.29	1.33	1.57	1.68
475021	47.00	5.00	21.00	449.71	39.10	9.56	10.20	4.61	4.58	1.52	1.54	21.20	19.60	1.18	1.25	1.41	1.56
476025	47.00	6.00	25.00	451.25	59.00	14.30	13.60	9.30	8.87	2.30	2.16	0.97	0.94	1.33	1.27	3.39	3.24
481007	48.00	1.00	7.00	453.27	—	3.21	3.21	—	37.18	—	3.65	—	6.16	—	0.39	—	0.58
481030	48.00	1.00	30.00	453.50	50.00	11.90	12.47	9.20	8.72	2.11	2.16	9.24	8.96	1.51	1.48	2.38	2.52
482034	48.00	2.00	34.00	455.04	40.80	9.97	10.58	4.36	4.15	1.62	1.61	20.40	19.60	1.29	1.28	1.32	1.44
483029	48.00	3.00	29.00	456.49	52.80	11.30	11.71	6.09	5.72	1.88	1.83	10.60	10.22	1.34	1.35	1.71	1.80
484032	48.00	4.00	32.00	458.02	48.90	11.30	12.09	4.68	4.58	1.79	1.83	13.70	12.88	1.15	1.28	1.53	1.68
485030	48.00	5.00	30.00	459.50	58.30	12.50	12.85	5.70	5.43	2.03	1.99	6.34	6.02	1.43	1.35	1.76	1.80
491074	49.00	1.00	74.00	463.54	47.40	11.40	12.09	4.66	4.58	1.94	1.99	14.20	13.44	1.31	1.48	1.55	1.68
492066	49.00	2.00	66.00	464.96	48.20	11.30	11.90	4.71	4.72	1.87	1.83	13.80	13.30	1.34	1.35	1.52	1.68
493080	49.00	3.00	80.00	466.60	33.40	7.80	8.31	8.23	8.01	2.09	2.16	17.30	16.80	1.07	1.23	0.95	1.20
494039	49.00	4.00	39.00	467.69	37.60	8.81	9.45	5.81	5.72	1.75	1.83	18.80	18.20	1.16	1.28	1.27	1.44
496043	49.00	6.00	43.00	470.73	40.60	7.97	8.69	3.48	3.43	1.36	1.43	22.60	22.40	1.16	1.16	1.05	1.20
501056	50.00	1.00	56.00	473.06	43.70	10.10	10.58	4.75	4.43	1.80	1.83	17.10	16.80	1.19	1.29	1.44	1.56
502056	50.00	2.00	56.00	474.56	45.20	10.50	11.15	5.29	4.86	1.84	1.83	15.60	15.40	1.09	1.31	1.60	1.68
503036	50.00	3.00	36.00	475.86	46.30	11.00	11.52	4.59	4.29	1.82	1.83	15.60	15.40	1.24	1.33	1.53	1.56
504032	50.00	4.00	32.00	477.32	29.40	6.46	6.99	9.50	9.58	2.02	2.16	17.60	16.80	0.89	1.13	0.77	1.09
505033	50.00	5.00	33.00	478.83	62.60	13.00	13.22	6.80	6.72	2.07	1.99	2.55	2.52	1.37	1.35	2.48	2.52
506012	50.00	6.00	12.00	480.12	30.70	6.88	7.37	10.60	10.58	2.14	2.16	14.60	13.86	0.87	1.02	1.08	1.20
511031	51.00	1.00	31.00	482.40	46.30	10.70	11.33	4.95	4.86	1.80	1.83	15.80	15.40	1.26	1.28	1.64	1.68
512036	51.00	2.00	36.00	483.96	38.00	8.85	9.45	4.17	4.15	1.58	1.58	21.30	19.60	1.06	1.13	1.15	1.32
513035	51.00	3.00	35.00	485.45	39.30	8.96	9.63	4.16	4.00	1.55	1.59	21.50	21.00	1.11	1.16	1.23	1.44
514068	51.00	4.00	68.00	487.28	4.84	1.10	1.25	16.40	17.16	2.47	2.66	18.90	18.20	0.33	0.65	0.07	0.17
515024	51.00	5.00	24.00	488.34	43.50	10.20	10.77	6.60	6.15	2.00	1.99	14.20	13.44	1.28	1.28	1.61	1.68
516083	51.00	6.00	83.00	490.41	—	—	3.40	—	18.59	—	3.15	—	12.60	—	0.65	—	0.48
522010	52.00	2.00	10.00	493.40	31.30	7.09	7.56	8.38	7.86	1.99	1.99	19.70	18.20	0.92	1.06	0.92	1.10
523098	52.00	3.00	98.00	495.78	38.70	6.89	7.56	5.74	5.86	1.67	1.66	19.80	19.60	1.06	1.15	0.97	1.16
524056	52.00	4.00	56.00	496.86	38.20	8.34	9.07	3.85	3.86	1.40	1.48	23.50	22.40	1.03	1.12	1.18	1.44
525069	52.00	5.00	69.00	498.49	36.80	9.24	10.01	5.22	5.15	1.68	1.66	21.20	19.60	0.94	1.11	1.31	1.56
526076	52.00	6.00	76.00	500.06	59.20	14.00	14.36	9.81	9.87	2.45	2.32	1.34	1.36	1.24	1.32	3.23	3.24
531047	53.00	1.00	47.00	501.87	44.90	10.90	11.52	5.10	5.01	1.80	1.83	16.20	15.40	1.22	1.27	1.66	1.80
532008	53.00	2.00	8.00	502.98	60.00	14.10	14.36	8.79	9.01	2.27	2.32	0.77	0.80	1.33	1.29	2.72	2.76
533055	53.00	3.00	55.00	504.95	47.20	10.20	10.77	5.52	5.29	1.73	1.83	14.90	14.00	1.22	1.23	1.67	1.80
534079	53.00	4.00	79.00	506.45	—	—	2.27	—	17.16	—	2.66	—	15.40	—	0.81	—	0.32
535018	53.00	5.00	18.00	507.58	42.30	9.90	10.39	5.41	5.15	1.67	1.66	18.50	18.20	1.10	1.15	1.55	1.68
541025	54.00	1.00	25.00	511.35	38.10	9.45	10.01	8.89	8.44	2.06	2.16	15.40	14.00	1.00	1.17	1.39	1.44
542013	54.00	2.00	13.00	512.73	40.30	9.04	9.82	5.43	5.43	1.69	1.83	19.00	18.20	1.09	1.19	1.29	1.44
543016	54.00	3.00	16.00	514.26	49.00	12.40	13.03	6.30	6.15	1.98	1.99	11.50	10.92	1.25	1.32	2.01	2.16
544123	54.00	4.00	123.00	516.83	60.40	13.00	13.41	9.63	9.72	2.18	2.16	2.60	2.66	1.14	1.19	2.72	2.88
545011	54.00	5.00	11.00	517.20	50.30	11.10	11.71	4.90	4.86	1.81	1.83	12.60	12.04	1.21	1.24	1.61	1.68
546014	54.00	6.00	14.00	518.74	40.40	8.19	8.69	3.61	3.72	1.33	1.39	22.40	21.00	1.03	1.06	1.08	1.20

443087	44.00	3.00	87.00	418.36	0.42	0.35	0.09	0.09	0.35	0.31	20.90	730.00	61.00	14.00	55.00	52.00	15.00	28.00
444116	44.00	4.00	116.00	420.16	0.36	0.33	0.09	0.09	0.33	0.31	23.80	680.00	49.00	14.00	59.00	37.00	14.00	23.00
445074	44.00	5.00	74.00	421.24	0.31	0.27	0.10	0.09	0.31	0.30	26.90	500.00	44.00	14.00	43.00	31.00	12.00	21.00
446064	44.00	6.00	64.00	422.64	0.38	0.33	0.06	0.07	0.23	0.22	24.00	550.00	52.00	23.00	54.00	41.00	14.00	24.00
451102	45.00	1.00	102.00	425.11	0.38	0.33	0.07	0.07	0.07	0.08	20.50	850.00	58.00	23.00	62.00	57.00	15.00	24.00
453055	45.00	3.00	55.00	427.65	0.35	0.30	0.07	0.07	0.08	0.09	21.10	790.00	52.00	100.00	63.00	77.00	14.00	23.00
461047	46.00	1.00	47.00	434.27	0.46	0.40	0.10	0.09	0.07	0.08	15.70	990.00	66.00	23.00	72.00	79.00	14.00	28.00
462041	46.00	2.00	41.00	435.71	0.39	0.35	0.08	0.07	0.08	0.09	18.80	1100.00	70.00	9.00	67.00	74.00	13.00	28.00
463041	46.00	3.00	41.00	437.21	0.45	0.38	0.10	0.09	0.07	0.07	16.30	1100.00	68.00	310.00	74.00	81.00	13.00	28.00
464041	46.00	4.00	41.00	438.71	0.57	0.50	0.08	0.07	0.05	0.06	13.30	720.00	70.00	18.00	83.00	85.00	15.00	29.00
465057	46.00	5.00	57.00	440.37	0.52	0.43	0.10	0.09	0.09	0.09	14.90	700.00	70.00	27.00	77.00	88.00	15.00	29.00
465111	46.00	5.00	111.00	440.91	0.31	0.22	11.30	12.37	0.23	0.22	14.50	730.00	860.00	15.00	48.00	69.00	11.00	410.00
466057	46.00	6.00	57.00	441.87	0.50	0.43	0.09	0.09	0.08	0.08	16.20	650.00	72.00	23.00	74.00	86.00	15.00	29.00
471033	47.00	1.00	33.00	443.82	0.47	0.42	0.08	0.07	0.09	0.10	15.80	810.00	45.00	14.00	80.00	36.00	14.00	20.00
473016	47.00	3.00	16.00	446.66	0.50	0.42	0.10	0.09	0.07	0.07	14.80	840.00	73.00	45.00	76.00	74.00	15.00	30.00
474021	47.00	4.00	21.00	448.21	0.46	0.40	0.07	0.07	0.30	0.28	16.70	770.00	66.00	33.00	70.00	78.00	16.00	28.00
475021	47.00	5.00	21.00	449.71	0.35	0.30	0.07	0.07	0.07	0.08	20.80	780.00	46.00	14.00	59.00	52.00	12.00	21.00
476025	47.00	6.00	25.00	451.25	0.51	0.40	0.08	0.07	0.03	0.04	8.38	820.00	130.00	34.00	96.00	130.00	15.00	55.00
481007	48.00	1.00	7.00	453.27	—	0.10	—	0.09	—	11.48	—	260.00	36.00	32.00	21.00	18.00	—	17.00
481030	48.00	1.00	30.00	453.50	0.44	0.38	0.07	0.07	0.24	0.23	13.20	1000.00	66.00	18.00	68.00	57.00	15.00	30.00
482034	48.00	2.00	34.00	455.04	0.38	0.33	0.08	0.09	0.07	0.08	20.20	590.00	58.00	22.00	59.00	75.00	12.00	25.00
483029	48.00	3.00	29.00	456.49	0.44	0.37	0.07	0.07	0.04	0.05	13.20	890.00	68.00	59.00	71.00	39.00	14.00	29.00
484032	48.00	4.00	32.00	458.02	0.46	0.40	0.13	0.11	0.12	0.12	15.40	830.00	78.00	51.00	70.00	73.00	16.00	30.00
485030	48.00	5.00	30.00	459.50	0.51	0.43	0.07	0.07	0.04	0.05	10.70	580.00	93.00	140.00	76.00	63.00	16.00	37.00
491074	49.00	1.00	74.00	463.54	0.44	0.38	0.12	0.11	0.58	0.52	16.20	870.00	57.00	32.00	70.00	64.00	18.00	24.00
492066	49.00	2.00	66.00	464.96	0.44	0.38	0.08	0.09	0.09	0.09	16.10	630.00	62.00	50.00	69.00	78.00	15.00	26.00
493080	49.00	3.00	80.00	466.60	0.31	0.27	0.12	0.11	5.81	5.55	22.90	570.00	76.00	26.00	44.00	53.00	31.00	31.00
494039	49.00	4.00	39.00	467.69	0.32	0.28	0.11	0.09	2.61	2.58	21.70	780.00	69.00	100.00	47.00	55.00	27.00	28.00
496043	49.00	6.00	43.00	470.73	0.27	0.25	0.07	0.07	0.17	0.17	21.10	630.00	36.00	25.00	48.00	58.00	10.00	16.00
501056	50.00	1.00	56.00	473.06	0.37	0.32	0.15	0.14	0.82	0.72	18.20	810.00	67.00	15.00	51.00	61.00	15.00	27.00
502056	50.00	2.00	56.00	474.56	0.40	0.33	0.06	0.07	0.10	0.10	18.00	610.00	52.00	45.00	62.00	84.00	12.00	23.00
503036	50.00	3.00	36.00	475.86	0.41	0.35	0.07	0.07	0.09	0.09	17.00	830.00	58.00	23.00	66.00	110.00	13.00	25.00
504032	50.00	4.00	32.00	477.32	0.23	0.20	2.01	2.04	7.86	7.74	23.30	2100.00	160.00	31.00	41.00	50.00	—	62.00
505033	50.00	5.00	33.00	478.83	0.47	0.38	0.08	0.07	0.06	0.06	8.41	640.00	87.00	36.00	90.00	68.00	16.00	37.00
506012	50.00	6.00	12.00	480.12	0.24	0.22	0.15	0.14	9.58	9.42	23.30	720.00	97.00	16.00	39.00	57.00	—	38.00
511031	51.00	1.00	31.00	482.40	0.40	0.35	0.07	0.07	0.23	0.22	17.00	1000.00	58.00	19.00	66.00	110.00	14.00	26.00
512036	51.00	2.00	36.00	483.96	0.30	0.27	0.10	0.09	0.80	0.70	22.30	840.00	53.00	23.00	52.00	65.00	16.00	23.00
513035	51.00	3.00	35.00	485.45	0.32	0.28	0.06	0.07	0.21	0.21	19.60	670.00	57.00	47.00	55.00	62.00	11.00	25.00
514068	51.00	4.00	68.00	487.28	0.04	0.05	7.31	8.24	20.20	19.35	27.70	3200.00	620.00	16.00	17.00	8.00	—	220.00
515024	51.00	5.00	24.00	488.34	0.37	0.33	0.12	0.11	2.37	2.45	18.20	940.00	53.00	21.00	60.00	50.00	18.00	23.00
516083	51.00	6.00	83.00	490.43	—	0.08	—	0.55	—	15.48	—	490.00	120.00	39.00	20.00	14.00	—	45.00
522010	52.00	2.00	10.00	493.40	0.24	0.22	0.78	0.80	5.48	5.29	24.00	610.00	110.00	14.00	44.00	160.00	14.00	44.00
523098	52.00	3.00	98.00	495.78	0.22	0.20	0.11	0.11	3.28	3.22	22.30	780.00	45.00	11.00	44.00	59.00	—	19.00
524056	52.00	4.00	56.00	496.86	0.30	0.27	0.08	0.09	0.13	0.13	22.40	700.00	59.00	70.00	55.00	71.00	12.00	24.00
525069	52.00	5.00	69.00	498.49	0.34	0.30	0.10	0.09	1.67	1.68	21.70	730.00	55.00	23.00	41.00	69.00	—	24.00
526076	52.00	6.00	76.00	500.06	0.48	0.42	0.06	0.07	0.03	0.04	8.10	720.00	110.00	18.00	97.00	71.00	17.00	44.00
531047	53.00	1.00	47.00	501.87	0.42	0.37	0.11	0.09	0.15	0.15	17.30	620.00	78.00	17.00	54.00	97.00	15.00	32.00
532008	53.00	2.00	8.00	502.98	0.50	0.43	0.06	0.07	0.021	0.03	8.81	650.00	86.00	86.00	94.00	50.00	17.00	38.00
533055	53.00	3.00	55.00	504.95	0.38	0.32	0.07	0.07	0.13	0.13	16.60	580.00	48.00	190.00	60.00	70.00	13.00	22.00
534079	53.00	4.00	79.00	506.45	—	0.05	—	7.56	—	16.77	—	1700.00	600.00	61.00	18.00	21.00	—	180.00
535018	53.00	5.00	18.00	507.58	0.39	0.33	0.09	0.09	0.18	0.17	18.60	590.00	59.00	62.00	52.00	75.00	12.00	26.00
541025	54.00	1.00	25.00	511.35	0.39	0.33	0.19	0.18	3.24	3.22	19.70	690.00	70.00	19.00	57.00	51.00	19.00	28.00
542013	54.00	2.00	13.00	512.73	0.35	0.32	0.09	0.09	1.36	1.12	20.10	680.00	44.00	27.00	59.00	80.00	19.00	19.00
543016	54.00	3.00	16.00	514.26	0.54	0.47	0.09	0.09	0.08	0.08	14.00	670.00	77.00	35.00	80.00	78.00	17.00	32.00
544123	54.00	4.00	123.00	516.83	0.45	0.40	0.06	0.05	0.03	0.04	7.80	760.00	110.00	21.00	83.00	61.00	18.00	43.00
545011	54.00	5.00	11.00	517.20	0.48	0.42	0.11	0.09	0.54	0.49	14.60	640.00	70.00	21.00	73.00	64.00	17.00	29.00
546014	54.00	6.00	14.00	518.74	0.30	0.28	0.11	0.09	0.20	0.19	21.10	610.00	50.00	19.00	48.00	46.00	11.00	21.00

443087	44.00	3.00	87.00	418.36	29.00	5.00	22.00	43.00	18.00	11.00	740.00	8.00	99.00	14.00	2.00	73.00	38.93	36.50
444116	44.00	4.00	116.00	420.16	28.00	7.00	18.00	43.00	11.00	10.00	890.00	8.00	89.00	13.00	1.00	52.00	45.71	43.92
445074	44.00	5.00	74.00	421.24	24.00	< 4.00	17.00	31.00	10.00	8.00	950.00	7.00	83.00	13.00	1.00	52.00	53.39	50.17
446064	44.00	6.00	64.00	422.64	25.00	5.00	17.00	43.00	12.00	9.00	890.00	7.00	85.00	10.00	1.00	54.00	45.36	43.00
451102	45.00	1.00	102.00	425.11	28.00	5.00	21.00	54.00	13.00	11.00	760.00	8.00	110.00	14.00	2.00	91.00	36.61	34.75
453055	45.00	3.00	55.00	427.65	27.00	4.00	19.00	54.00	14.00	11.00	800.00	7.00	110.00	13.00	1.00	88.00	39.82	34.08
461047	46.00	1.00	47.00	434.27	31.00	6.00	27.00	68.00	17.00	12.00	530.00	9.00	150.00	19.00	2.00	75.00	25.00	22.75
462041	46.00	2.00	41.00	435.71	29.00	5.00	25.00	43.00	18.00	11.00	760.00	8.00	170.00	16.00	2.00	44.00	34.11	32.08
463041	46.00	3.00	41.00	437.21	30.00	< 4.00	29.00	77.00	19.00	12.00	510.00	11.00	140.00	18.00	2.00	65.00	24.64	21.67
464041	46.00	4.00	41.00	438.71	35.00	7.00	29.00	49.00	19.00	14.00	390.00	9.00	220.00	16.00	2.00	100.00	17.75	16.17
465057	46.00	5.00	57.00	440.37	31.00	7.00	27.00	78.00	22.00	12.00	490.00	9.00	160.00	14.00	2.00	80.00	23.75	21.92
465111	46.00	5.00	111.00	440.91	20.00	5.00	280.00	47.00	14.00	14.00	910.00	< 4.00	110.00	430.00	24.00	62.00	50.18	21.92
466057	46.00	6.00	57.00	441.87	31.00	9.00	27.00	71.00	16.00	12.00	520.00	10.00	160.00	16.00	2.00	100.00	25.36	23.33
471033	47.00	1.00	33.00	443.82	32.00	7.00	18.00	55.00	18.00	12.00	490.00	9.00	160.00	11.00	1.00	50.00	23.39	22.00
473016	47.00	3.00	16.00	446.66	33.00	6.00	28.00	46.00	16.00	13.00	450.00	10.00	160.00	18.00	2.00	88.00	21.79	19.83
474021	47.00	4.00	21.00	448.21	32.00	7.00	26.00	53.00	12.00	14.00	550.00	11.00	160.00	17.00	2.00	110.00	24.46	25.00
475021	47.00	5.00	21.00	449.71	27.00	6.00	18.00	40.00	14.00	10.00	780.00	9.00	120.00	15.00	2.00	56.00	37.86	35.75
476025	47.00	6.00	25.00	451.25	37.00	8.00	54.00	86.00	27.00	12.00	150.00	17.00	290.00	27.00	3.00	100.00	1.73	0.75
481007	48.00	1.00	7.00	453.27	14.00	< 4.00	13.00	26.00	6.00	4.00	120.00	< 4.00	41.00	17.00	2.00	69.00	11.00	69.75
481030	48.00	1.00	30.00	453.50	41.00	6.00	26.00	59.00	18.00	13.00	410.00	11.00	170.00	13.00	2.00	73.00	16.50	15.67
482034	48.00	2.00	34.00	455.04	31.00	< 4.00	24.00	48.00	11.00	11.00	730.00	6.00	140.00	17.00	2.00	110.00	36.43	34.00
483029	48.00	3.00	29.00	456.49	36.00	6.00	26.00	90.00	19.00	13.00	440.00	8.00	130.00	15.00	2.00	69.00	18.93	16.75
484032	48.00	4.00	32.00	458.02	35.00	6.00	28.00	78.00	20.00	13.00	530.00	9.00	130.00	19.00	2.00	99.00	24.46	22.08
485030	48.00	5.00	30.00	459.50	37.00	6.00	34.00	81.00	20.00	14.00	310.00	11.00	140.00	15.00	2.00	110.00	11.32	9.83
491074	49.00	1.00	74.00	463.54	32.00	6.00	24.00	54.00	17.00	13.00	560.00	11.00	140.00	17.00	2.00	92.00	25.36	23.75
492066	49.00	2.00	66.00	464.96	31.00	6.00	24.00	67.00	17.00	12.00	590.00	9.00	160.00	15.00	2.00	100.00	24.64	22.57
493080	49.00	3.00	80.00	466.60	24.00	5.00	27.00	38.00	10.00	10.00	600.00	18.00	100.00	21.00	3.00	62.00	30.89	41.83
494039	49.00	4.00	39.00	467.69	25.00	5.00	26.00	79.00	21.00	10.00	670.00	13.00	120.00	18.00	2.00	61.00	33.57	35.00
496043	49.00	6.00	43.00	470.73	28.00	< 4.00	12.00	49.00	11.00	9.00	790.00	6.00	110.00	10.00	1.00	83.00	43.36	38.33
501056	50.00	1.00	56.00	473.06	28.00	5.00	30.00	43.00	14.00	11.00	620.00	7.00	120.00	20.00	2.00	81.00	30.54	29.67
502056	50.00	2.00	56.00	474.56	29.00	5.00	21.00	71.00	20.00	12.00	580.00	9.00	140.00	12.00	2.00	92.00	27.86	25.25
503036	50.00	3.00	36.00	475.86	30.00	4.00	23.00	56.00	18.00	12.00	580.00	9.00	170.00	12.00	1.00	120.00	27.86	24.75
504032	50.00	4.00	32.00	477.32	21.00	4.00	67.00	47.00	10.00	9.00	640.00	< 4.00	95.00	82.00	5.00	73.00	31.43	43.83
505033	50.00	5.00	33.00	478.83	38.00	6.00	32.00	59.00	20.00	12.00	190.00	14.00	190.00	11.00	1.00	80.00	4.55	3.42
506012	50.00	6.00	12.00	480.12	22.00	< 4.00	34.00	48.00	12.00	9.00	500.00	4.00	100.00	30.00	4.00	85.00	26.07	43.92
511031	51.00	1.00	31.00	482.40	29.00	5.00	23.00	58.00	16.00	11.00	630.00	10.00	160.00	13.00	2.00	120.00	28.21	25.33
512036	51.00	2.00	36.00	483.96	24.00	4.00	24.00	52.00	14.00	10.00	820.00	8.00	120.00	16.00	2.00	87.00	38.04	36.08
513035	51.00	3.00	35.00	485.45	25.00	6.00	23.00	61.00	13.00	10.00	780.00	8.00	110.00	13.00	2.00	76.00	38.39	34.58
514068	51.00	4.00	68.00	487.28	9.00	< 4.00	300.00	15.00	< 4.00	7.00	760.00	43.00	28.00	300.00	16.00	85.00	33.75	63.92
515024	51.00	5.00	24.00	488.34	27.00	5.00	24.00	59.00	16.00	11.00	520.00	8.00	120.00	20.00	2.00	54.00	25.36	28.00
516083	51.00	6.00	83.00	490.43	15.00	< 4.00	57.00	39.00	8.00	7.00	350.00	< 4.00	59.00	54.00	5.00	38.00	22.50	65.67
522010	52.00	2.00	10.00	493.40	23.00	< 4.00	48.00	29.00	19.00	9.00	730.00	< 4.00	150.00	49.00	3.00	300.00	35.18	45.83
523098	52.00	3.00	98.00	495.78	29.00	< 4.00	17.00	23.00	8.00	7.00	730.00	5.00	93.00	18.00	2.00	33.00	35.36	41.17
524056	52.00	4.00	56.00	496.86	26.00	< 4.00	21.00	35.00	10.00	9.00	910.00	7.00	110.00	16.00	2.00	51.00	41.96	39.08
525069	52.00	5.00	69.00	498.49	24.00	4.00	22.00	51.00	14.00	10.00	790.00	8.00	130.00	20.00	2.00	75.00	37.86	39.25
526076	52.00	6.00	76.00	500.06	34.00	8.00	41.00	58.00	18.00	13.00	170.00	17.00	260.00	14.00	2.00	83.00	2.39	1.50
531047	53.00	1.00	47.00	501.87	28.00	5.00	30.00	60.00	28.00	12.00	670.00	10.00	160.00	18.00	2.00	110.00	28.93	26.08
532008	53.00	2.00	8.00	502.98	36.00	10.00	33.00	51.00	10.00	13.00	150.00	17.00	230.00	12.00	2.00	65.00	1.38	0.42
533055	53.00	3.00	55.00	504.95	30.00	5.00	19.00	260.00	24.00	11.00	580.00	8.00	150.00	12.00	1.00	68.00	26.61	24.25
534079	53.00	4.00	79.00	506.45	10.00	< 4.00	340.00	18.00	< 4.00	8.00	590.00	< 4.00	60.00	330.00	20.00	380.00	27.50	58.92
535018	53.00	5.00	18.00	507.58	27.00	< 4.00	26.00	62.00	14.00	11.00	680.00	7.00	130.00	16.00	2.00	82.00	33.04	30.42
541025	54.00	1.00	25.00	511.35	24.00	4.00	29.00	54.00	16.00	11.00	570.00	7.00	130.00	20.00	2.00	67.00	27.50	35.58
542013	54.00	2.00	13.00	512.73	27.00	5.00	15.00	70.00	14.00	10.00	730.00	7.00	120.00	13.00	2.00	68.00	33.93	30.75
543016	54.00	3.00	16.00	514.26	30.00	7.00	28.00	73.00	15.00	14.00	490.00	12.00	170.00	16.00	2.00	89.00	20.54	18.33
544123	54.00	4.00	123.00	516.83	38.00	7.00	38.00	75.00	20.00	13.00	190.00	19.00	190.00	12.00	2.00	70.00	4.64	3.67
545011	54.00	5.00	11.00	517.20	31.00	6.00	27.00	64.00	17.00	12.00	550.00	9.00	150.00	17.00	2.00	90.00	22.50	20.75
546014	54.00	6.00	14.00	518.74	25.00	4.00	19.00	41.00	14.00	9.00	840.00	7.00	110.00	14.00	1.00	68.00	40.00	37.92

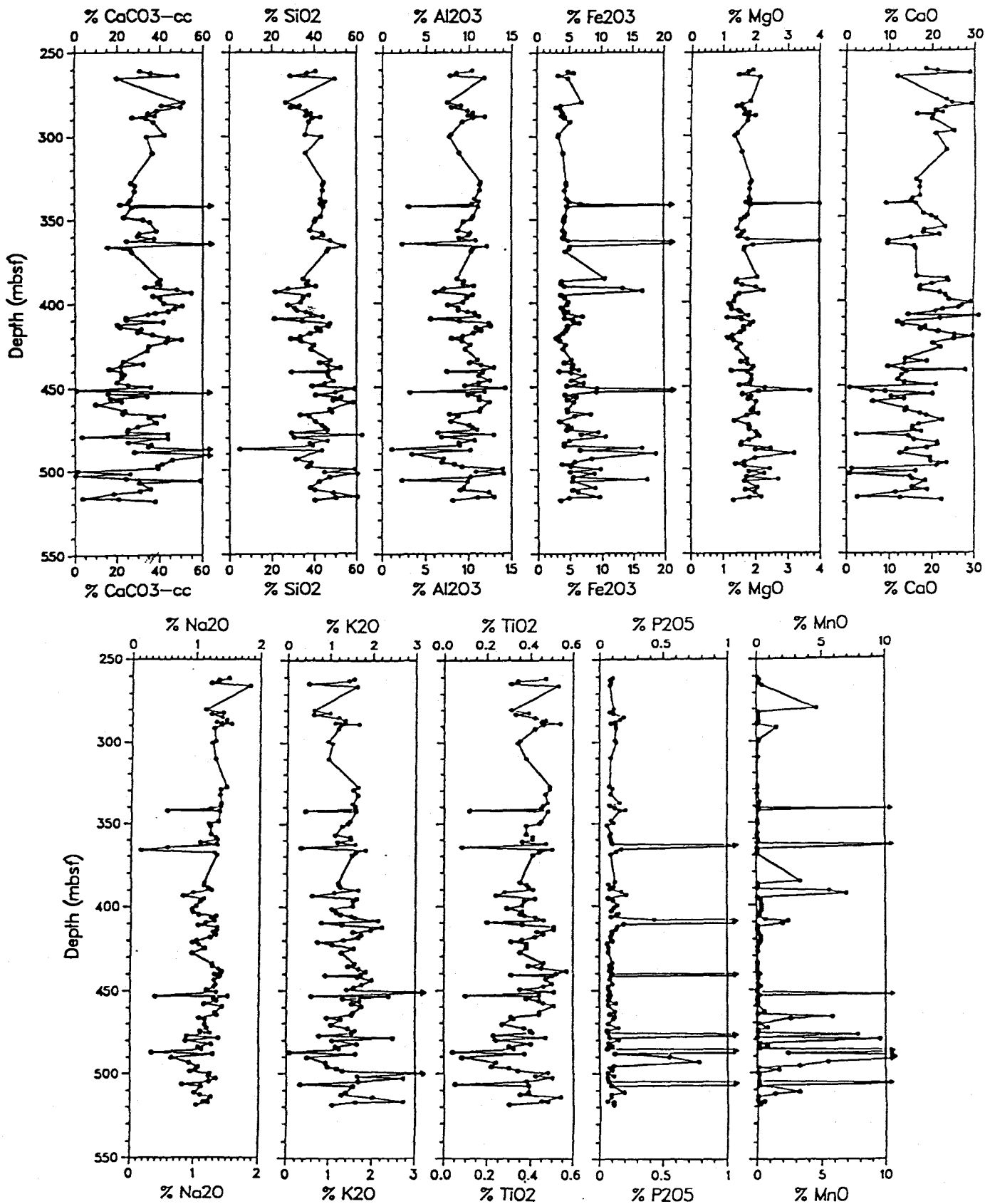


Figure 2. Concentrations of CaCO<sub>3</sub>, computed from carbonate carbon (CC) and major-element oxides in samples from lithologic Unit IIIc, Hole 647A.

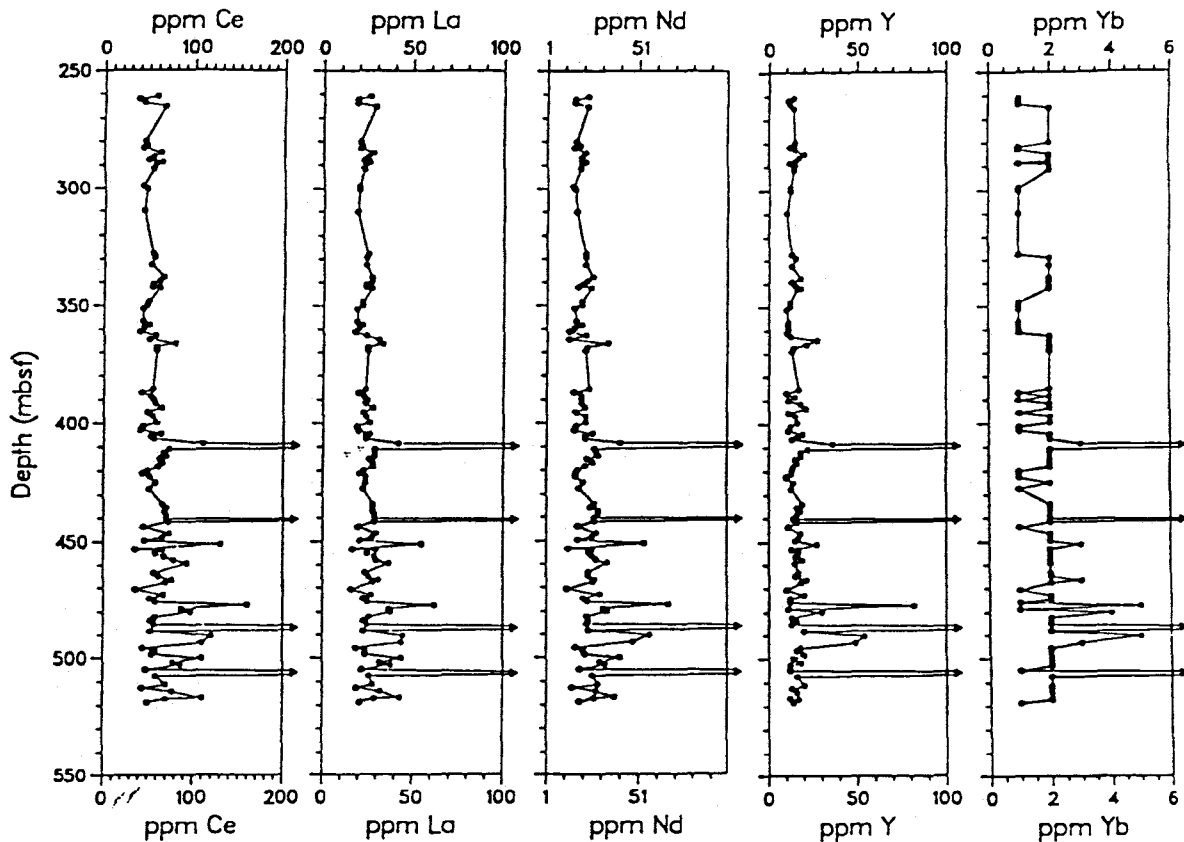


Figure 4. Concentrations of Ce, La, Nd, Y, and Yb in samples from lithologic Unit IIIC, Hole 647A.

dominated by four samples (although not the same four samples), with moderate loadings for a few other samples. The most important variables used to group factor IV samples are Mn, Fe, Mg, and LOI.

The raw data plots (Figs. 1 through 6), particularly the plots of factor loadings (Fig. 7), show that most samples from lithologic Unit IIIC consist mainly of detrital clastic material plus varying amounts of  $\text{CaCO}_3$ . That the clastic fraction is fairly typical of average crustal material is shown by Table 3, which compares the carbonate-free concentrations of elements in a typical sample from Unit IIIC (Sample 36-4-68) with those in average crust and average deep-sea clay. The most striking features of the downhole plots, however, are the horizons having distinctly different chemical characteristics because of high concentrations of one or more REE-bearing phosphate minerals and/or high concentrations of one or more Mn-, Fe-, and Mg-bearing minerals. Results of the Ca and CC analyses show that the phosphate mineral is indeed calcium phosphate (carbonate-fluorapatite as determined by X-ray diffraction [XRD], Tables 4 and 5) and the Mn-, Fe-, and Mg-bearing minerals are one or more phases of carbonate, which XRD analysis confirmed was rhodochrosite, siderite, and manganosiderite. We mentioned earlier that for most deep-sea carbonate sediments or rocks we obtain essentially identical results for the percentage of  $\text{CaCO}_3$  calculated from total Ca and from CC. For the Site 647 samples, however, neither method gives correct results for all samples because of excess Ca from the apatite and excess CC from Mn-Fe-Mg carbonate. The difference between the two methods is shown in Figures 8 and 9. Figure 9 is a downhole plot of  $\text{CaCO}_3$  computed from CC— $\text{CaCO}_3$  computed from Ca. The

differences plotted in Figure 9 and the analytical results can be used to calculate the amount of apatite present, and the amount and molar proportions of cations in the Mn-Fe-Mg carbonate. For example, Sample 43-4-25 (409.55 mbsf) contains 31.3%  $\text{CaO}$  (= 22.4% Ca), 14.8%  $\text{P}_2\text{O}_5$  (= 6.45% P), and 2.9% CC. Assuming that all of the P is in simple calcium fluorapatite ( $\text{Ca}_5\text{F}[\text{PO}_4]_3$ ) with a molar Ca:P ratio of 1.67, then 14.0% Ca is in apatite, and the amount of apatite in the sample is 35%. If all of the residual Ca (8.4%) is assumed to be in calcite, then the computed percentage of  $\text{CaCO}_3$  is 21%, which compares with 24% computed from CC.

As an example of a Mn-Fe-Mg carbonate, Sample 38-6-67 (364.6 mbsf) contains 31.5%  $\text{Fe}_2\text{O}_3$  (22% Fe), 12.9% MnO (10% Mn), 6.9%  $\text{CaO}$  (6.9% Ca), 1.6%  $\text{P}_2\text{O}_5$  (0.7% P), and 8.55% CC. Assuming that all of the P is in apatite with a Ca:P ratio of 1.67, and all of the residual Ca and all of the Mg, Mn, and Fe are in one carbonate mineral, then the formula for this carbonate mineral is:



Most of the other Fe- and Mn-rich samples have similar molar proportions of the four divalent cations.

The occurrence of these apparently authigenic carbonate and phosphate minerals seems anomalous for a primarily pelagic sedimentary sequence. However, the relatively high sedimentation rate (about 36 m/m.y.) over part of the sequence is more indicative of a hemipelagic regime, one in which suboxic to anoxic early diagenesis could induce substantial redistribution of organic-associated and redox-sensitive elements. In addition, there

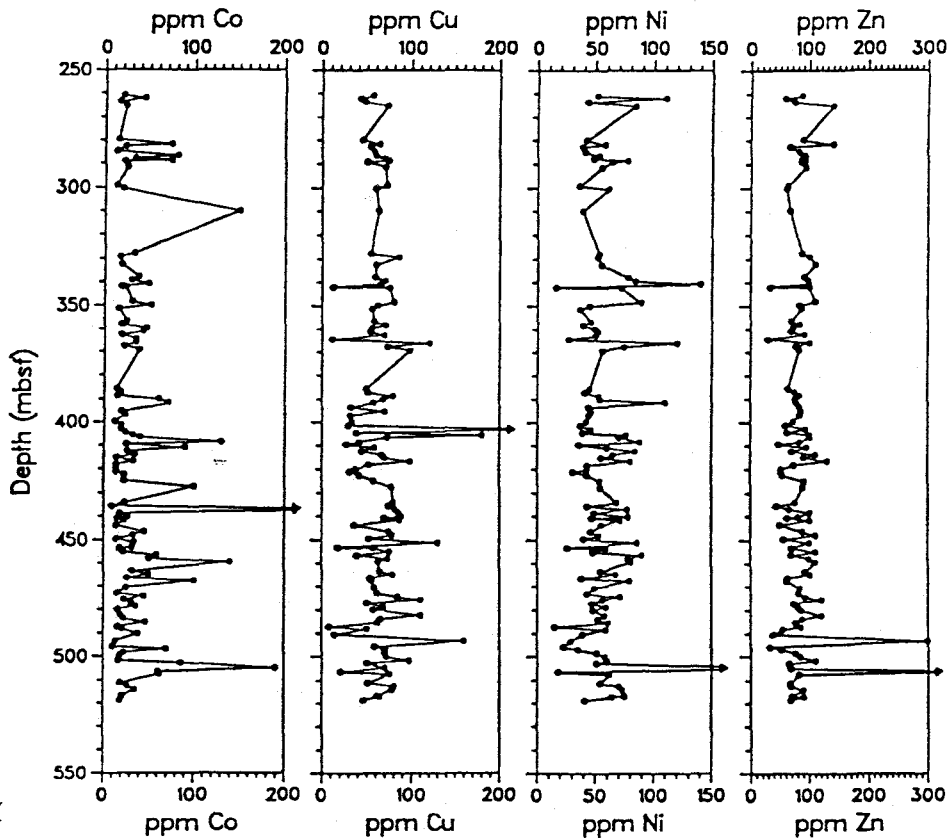


Figure 6. Concentrations of Co, Cu, Ni, and Zn in samples from lithologic Unit IIIC, Hole 647A.

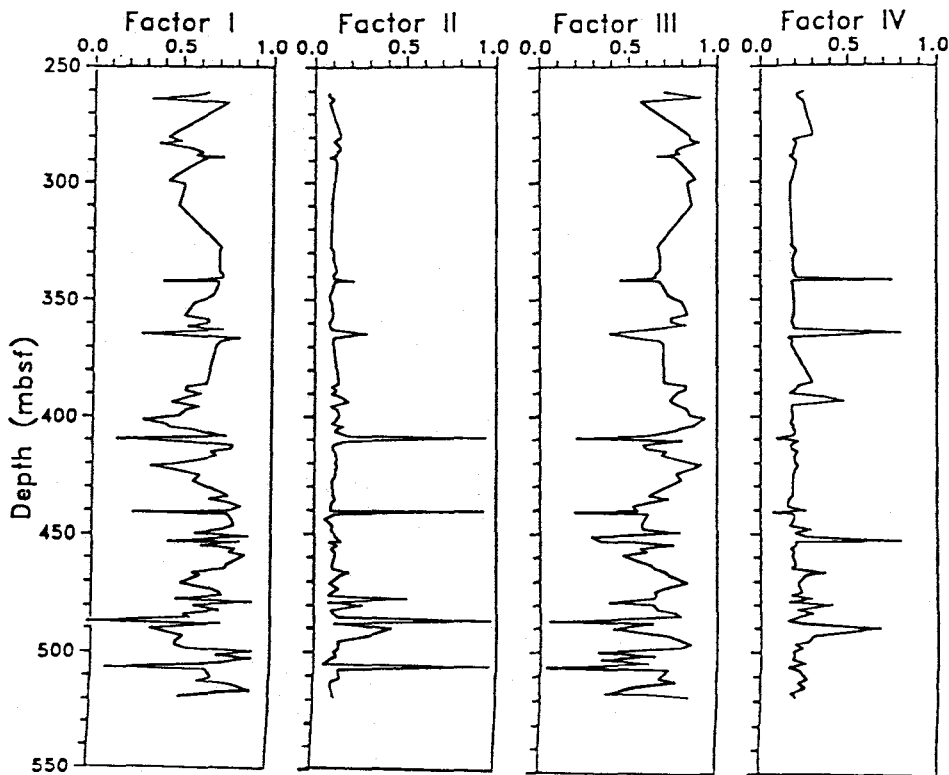


Figure 7. Plots of factor loadings from a four-factor Q-mode factor analysis of element concentrations in samples from lithologic Unit IIIC, Hole 647A.

Table 5. Whole-sediment (concretions or layers) XRD results.

Core/section/ interval	Depth (mbsf)	Main minerals present	Comments	Fe <sub>2</sub> O <sub>3</sub> , MnO, P <sub>2</sub> O <sub>5</sub> (%)
105-647A-30-1, 51	279.93	Siderite-Rhodochrosite-Calcite		(not anomalous)
36-4, 42	342.13	Siderite-Manganosiderite	(broad peaks)	(31.5, 11.5, 0.21)
38-6, 67	364.56	Siderite-Manganosiderite	(broad peaks)	(31.5, 12.9, 1.56)
43-4, 25	409.55	Aparite-Calcite		(4.31, 2.42, 14.8)
46-5, 111	440.91	Aparite		(3.46, 0.23, 11.3)
48-1, 7	453.27	Siderite-Manganosiderite	(sharp peaks)	(37.2, 11.5, 0.55)
50-4, 32	477.32	Siderite-Rhodochrosite-Calcite		(9.5, 7.86, 2.01)
51-4, 68	487.28	Rhodochrosite-Siderite	(broad peaks)	(16.4, 20.2, 7.31)
51-6, 83	490.43	Siderite-Rhodochrosite-Calcite	(Calcite peak shift; Mg substitution)	(18.6, 15.5, 0.55)
52-2, 10	493.40	Calcite-(minor) Siderite		(not anomalous)
53-4, 79	506.45	Manganosiderite		(17.2, 16.7, 7.6)

Note: Diffractometer parameters: 1.2°2θ/min from 10 to 60°2θ with CuKα radiation.

Coulto  
COMPARISON

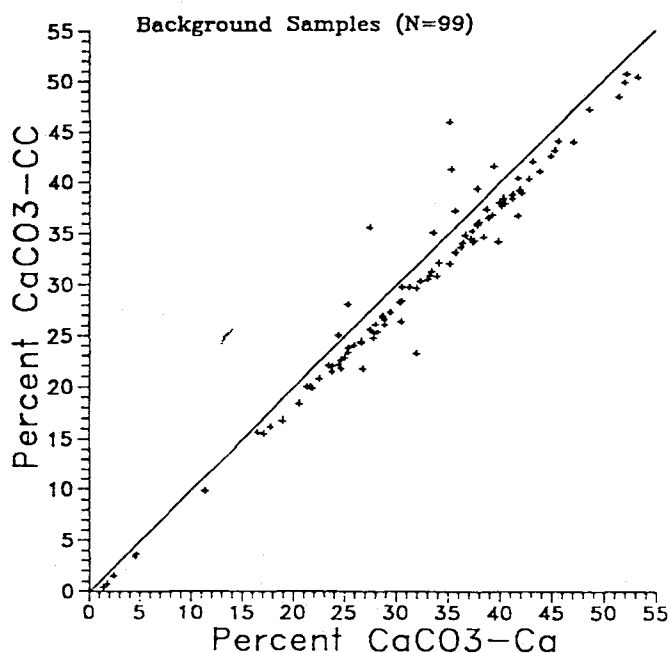


Figure 8. Plot of CaCO<sub>3</sub> of "background" (nonconcretionary) samples from Hole 647A calculated from carbonate carbon (coulometry, see text) vs. that calculated from Ca geochemical data. Note close agreement between two techniques, with the exception of a few points, which probably contain authigenic carbonate phases.

cur, the solution-susceptible planktonic tests may be the primary source of carbonate, while the interior and exterior walls of benthic tests are the selective sites for cement precipitation. Of the benthic foraminifers, *Oridorsalis* species and *Cibicidoides* consistently display the lightest values, suggesting that of the benthics these species provide the most favorable sites for cement precipitation.

**Carbon Isotopes**

As with the oxygen isotopes, the carbon isotopic composition of the planktonic foraminifers is little affected by diagenesis. Samples of both *C. unicavus* and *G. eoceana* have δ<sup>13</sup>C values of 0.50 to 0.75‰ from the middle Eocene, again with no discernable difference between the species. A slight decrease in δ<sup>13</sup>C can be measured from the middle to upper Eocene parts of the seafloor, where the average values of planktonic foraminifers are less than 0.25‰ (Fig. 11).

The carbon isotopic composition of the benthic foraminifers is progressively more negative from lower to upper Eocene at

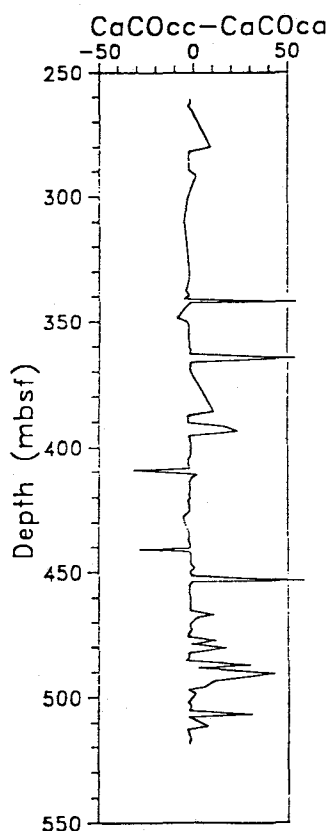


Figure 9. Plot of difference in CaCO<sub>3</sub> computed from carbonate carbon (CC) and from calcium for samples from lithologic Unit IIIC, Hole 647A.

Site 647 (Fig. 11). The measured δ<sup>13</sup>C values for all species range from -0.7 to +0.5‰ in the lower Eocene and from -2.0 to -0.3‰ in the upper Eocene, with *Oridorsalis* consistently yielding the lightest values. The carbon isotopic compositions of *Nuttallides* and *Cibicidoides* overlap upsection and are on average 1.0‰ heavier than those of *Oridorsalis*.

Comparatively heavier δ<sup>13</sup>C values, in the range of -0.25 to 1.5‰, have been reported for various species of benthic foraminifers from other Eocene pelagic sequences located in the equatorial Pacific (Keigwin, 1980), south Atlantic, eastern Indian Arabian Sea (Keigwin and Corliss, 1986), and the Bay of Biscay (Miller et al., 1985). In addition, the records at these locations give no indication of a depletion in the deep-water mass carbon isotopic composition during the middle to late Eocene.



**Table 6. Visual (microscopic) estimation of preservation of samples picked for benthic and planktonic foraminifers for stable-isotope analyses.**

Core, section interval (cm)	Depth (mbsf)	Benthic preservation	Comments	Planktonics
105-647A-28-1, 108-115	261.18	G		
28-2, 105-108	262.65	G		
28-3, 105-108	264.15	G		
28-4, 91-98	265.51	G		
28-4, 105-108	265.65	G		
30-1, 107-111	280.47	G		Few dwarf
30-2, 25-29	281.15	G		G
30-3, 110-114	283.54	G		G
30-4, 107-111	284.97	M/G	(Few pits, pyrite)	Few
30-5, 10-12	285.50	M/G	(Some etching, <i>Nuttallides</i> abundant)	
30-7, 33-38	288.73	M/G	(Some pyrite in- <i>Orid.</i> )	M/G
31-1, 132-136	299.92	M/G	(Signs of etching)	
31-2, 34-37	290.84	M/G	(Some etching)	
32-1, 84-93	299.44	M	(Stronger etching, <i>Orid.</i> /pyrite)	M
32-2, 20-24	300.30	M/G	(Some etching, <i>Gyrodin.</i> )	
33, CC	310.60	M/G	(No pyrite, some etching)	
34, CC	319.30	M/G	(No visible pyrite)	
35-1, 77-80	328.37	M/G	(Abund. pyrite on all forms)	
35-2, 77-80	329.87	M	(Pyrite; etching; broken spec.)	M/G
35-3, 77-80	331.37	M/G	(Better than above, no pyrite)	
36-2, 49-52	339.19	M	(Abund. pyrite, etching)	M low abund.
36-3, 49-52	340.69	M/G	(No pyrite, better than above)	
36-4, 49-52	342.19	M/G	(Pyrite present)	
37-2, 90-93	349.10	M	(Abund. pyrite)	
37-3, 90-93	350.60	P/M	(Abund. pyrite, etching frags.)	low abund.
37-4, 90-93	352.10	M/G	(Pyrite absent)	
38-1, 83-86	357.24	M	(Orange; some etching)	M/G abund.
38-2, 84-87	358.74	M/G	(Orange)	
38-3, 86-89	360.26	M/G	(Clear/White)	
38-4, 86-89	361.76	M/G	(No pyrite/clear)	
39-1, 80-83	366.90	M	(Orange/pyrite)	M
39-2, 77-80	368.37	M/G	(Low abund., trace pyrite)	(w/ppm)
39, CC	370.10	M	(Orange; pyrite abund.)	M (some pyr.)
41-1, 58-61	385.98	M/G	(White, some pyrite)	
41-3, 58-61	288.98	M	(White, no pyrite)	M/G
41-5, 58-61	391.98	M/G	(White, no pyrite)	
42-3, 32-35	398.42	M/G	(White, no pyrite)	
42-5, 96-100	402.06	M/G	(White, no pyrite)	
43-1, 95-98	405.75	M	(White, no pyrite)	
43-3, 104-108	408.84	M	(Some etching, no pyrite, white)	M/G
43-5, 97-100	411.77	M	(Dissolved, some pyrite)	
44-1, 45-48	414.95	M/G	(Some pyrite)	M/G
44-3, 42-46	417.92	M/G	(No pyrite)	
44-5, 45-48	420.95	G	(No pyrite, white, clear)	
45-1, 14-18	424.24	M/G	(No pyrite, some etching)	
45-2, 20-24	425.80	M/G	(No pyrite, some etching)	
46-1, 60-63	434.40	M	(Orange color, no pyrite)	
46-3, 60-63	437.40	M	(Orange color, no pyrite)	
46-5, 60-63	440.40	M	(Orange color, abund. pyrite)	
47-4, 74-74	448.74	M/G	(No pyrite, white)	
47-5, 55-58	450.05	M/G	(No pyrite, orange)	
47-6, 52-55	451.52	P	(Nearly barren)	
48-1, 100-109	454.20	M	(Orange, no pyrite)	
48-3, 107-110	457.27	M	(Orange, some pyrite)	M
48-5, 104-107	460.24	M	(Lt. orange, some pyrite)	
49-1, 118-121	463.98	M/G	(White, no pyrite)	
49-5, 117-120	469.97	M/G	(Orange tinge, white, no pyrite)	
49-6, 117	471.47	M/G	(White, no pyrite)	
50-1, 91-94	473.41	M/G	(Some pyrite, orange)	
50-3, 91-94	476.41	M	(White, no pyrite)	M
50-5, 44-46	478.94	M/G	(White, no pyrite)	
51-2	493.60	M	(Orange tinge, trace pyrite)	
51-4, 69-71	487.29	M/G	(Orange tinge, trace pyrite)	
51-5, 94-97	489.04	M/G	(Orange tinge, low abund., no pyrite)	
52-2, 45-48	493.75	M/G	(Orange tinge, low abund., no pyrite)	
52-3, 45-48	495.25	M	(Trace pyrite, white)	
52-5, 52-55	498.32	M/G	(White, no pyrite)	
53-2, 40-44	503.30	M	(Some pyrite, white)	
53-4, 84-87	505.24	M/G	(Orange, no pyrite)	
53-5, 24-26	507.74	M	(Slight orange tinge, no pyrite)	
54-2, 32-35	512.82	M	(Slight orange tinge, trace pyrite)	
54-6, 23-27	518.83	M/G	(White, no pyrite)	

Table 7. Stable-isotope results from planktonic and benthic foraminifers and bulk samples.

Core, section, interval (cm)	Species	Depth (m)	$\delta^{18}\text{O}$ (PDB)	$\delta^{13}\text{C}$ (PDB)
105-647A-25-2, 28-30	<i>Unicavus</i>	233.80	-0.38	-0.01
33cc	Mixed planks	308.30	-0.90	0.30
35cc	Mixed planks	327.60	-0.84	0.46
39-2, 16-18	<i>Eoceana</i>	367.60	-0.21	0.01
41-3, 29-31	<i>Unicavus</i>	388.69	-1.58	0.29
41-5, 29-31	<i>Unicavus</i>	391.69	-0.59	0.09
42cc	Mixed planks	395.10	-0.54	0.39
44-1, 79-81	<i>Unicavus</i>	415.29	-0.63	0.53
44-4, 115-117	<i>Eoceana</i>	420.15	-1.44	-0.45
44-4, 115-117	<i>Unicavus</i>	420.15	-1.84	0.07
45cc	Mixed planks	424.10	-0.85	0.37
46cc	Mixed planks	433.80	-1.15	0.23
46-2, 40-42	<i>Unicavus</i>	435.50	-1.41	0.34
46-2, 40-42	<i>Eoceana</i>	435.50	-1.78	0.26
46R, 2	<i>Unicavus</i>	436.80	-1.37	0.30
46R, 2	<i>Eoceana</i>	436.80	-0.84	0.41
46-3, 40-42	<i>Unicavus</i>	437.20	-1.36	0.39
46-4, 40-42	<i>Unicavus</i>	438.70	-1.06	0.74
47-5, 20-22	<i>Unicavus</i>	449.70	-1.67	0.58
47-5, 20-22	<i>Eoceana</i>	449.70	-1.80	0.75
51cc	<i>Eoceana</i>	482.10	-1.46	0.57
30-1, 107-109	<i>Oridorsalis</i>	280.47	0.72	-1.39
30-2, 25-27	<i>Oridorsalis</i>	281.15	0.49	-1.25
30-4, 107-109	<i>Oridorsalis</i>	284.97	0.28	-1.56
30-4, 107-109	<i>G. Subglobosa</i>	284.97	0.52	-1.46
31-1, 132-134	<i>Oridorsalis</i>	290.32	0.39	-1.76
31-1, 132-134	<i>G. Subglobosa</i>	290.32	0.49	-1.98
33cc	<i>Oridorsalis</i>	318.00	-1.35	-1.61
35-3, 77-79	<i>Oridorsalis</i>	331.37	-0.92	-0.97
36-2, 49-51	<i>Oridorsalis</i>	349.19	-1.86	-1.16
41-3, 58-61	<i>Cibicidoides</i>	388.98	-3.38	-0.71
41-3, 58-61	<i>Stilostomella</i>	388.98	-0.84	-0.62
41-5, 58-60	<i>Oridorsalis</i>	391.98	-3.47	-1.39
41-5, 58-60	<i>G. Subglobosa</i>	391.98	-1.96	-1.05
41-5, 58-61	<i>Cibicidoides</i>	391.98	-3.67	-0.70
42-3, 32-34	<i>Oridorsalis</i>	398.42	-2.07	-1.53
42-3, 32-34	<i>G. Subglobosa</i>	398.42	-1.24	-0.96
42-3, 33-35	<i>Cibicidoides</i>	398.43	-3.38	-0.90
41-3, 58-61	<i>Oridorsalis</i>	398.98	-4.13	-1.45
43-1, 95-97	<i>Oridorsalis</i>	405.75	-4.19	-1.61
43-1, 95-98	<i>Cibicidoides</i>	405.75	-4.04	-0.94
44-3, 24-26	<i>Oridorsalis</i>	417.74	-1.50	-1.31
44-3, 24-26	<i>G. Subglobosa</i>	417.74	-0.56	-1.42
44-3, 42-46	<i>Cibicidoides</i>	417.92	-0.88	-0.40
45-1, 14-16	<i>Oridorsalis</i>	424.24	-3.34	-1.43
45-1, 14-16	<i>Nuttalides</i>	424.24	-2.36	-0.62
45-1, 14-18	<i>Cibicidoides</i>	424.24	-3.71	-0.52
45-2, 20-22	<i>Oridorsalis</i>	425.80	-2.81	-1.33
45-2, 20-24	<i>Cibicidoides</i>	425.80	-2.34	-0.22
46-1, 60-62	<i>Oridorsalis</i>	434.40	-3.36	-1.43
47-5, 55-57	<i>Oridorsalis</i>	448.65	-1.32	-0.63
48-1, 106-108	<i>Oridorsalis</i>	454.26	-2.88	-1.28
48-5, 104-106	<i>Oridorsalis</i>	460.24	-3.61	-1.89
49-5, 117-119	<i>Oridorsalis</i>	469.97	-2.72	-1.76
49-6, 117-119	<i>Oridorsalis</i>	471.47	-2.48	-1.51
50-1, 91-93	<i>Oridorsalis</i>	473.41	-2.10	-1.22
50-5, 44-46	<i>Oridorsalis</i>	478.94	-1.39	-1.12
51-4, 69-71	<i>Oridorsalis</i>	487.29	-0.48	-1.17
51-5, 49-51	<i>Oridorsalis</i>	488.59	-1.08	-1.36
53-4, 84-87	<i>Oridorsalis</i>	506.74	-1.66	-1.21
53-5, 24-26	<i>Oridorsalis</i>	507.64	-2.43	-1.34
54-6, 23-27	<i>Oridorsalis</i>	518.83	-2.36	-1.48
54-6, 23-27	<i>Stilostemella</i>	518.83	-1.69	-1.13
54-6, 24-27	<i>Cibicidoides</i>	518.84	-2.25	-0.12
55cc	<i>Oridorsalis</i>	530.30	-2.63	-1.36
56cc	<i>Nuttalides</i>	540.00	-2.45	-1.06
60cc	<i>Oridorsalis</i>	578.80	-2.95	-1.16
60cc	<i>Nuttalides</i>	578.80	-2.70	-0.40
60cc	<i>Stilostemella</i>	578.80	-2.37	-0.93
61cc	<i>Oridorsalis</i>	586.90	-3.17	-0.57
61cc	<i>Oridorsalis</i>	588.40	-3.56	-1.22
61cc	<i>Nuttalides</i>	588.40	-3.35	-0.67
61cc	<i>Cibicidoides</i>	588.40	-3.72	-0.34
62-3, 60-63	<i>Nuttalides</i>	601.70	-2.61	-0.49
63-1, 139-141	<i>N. Trumpeyi</i>	609.19	-3.14	-0.55
66-3, 57-59	<i>N. Trumpeyi</i>	640.37	-2.40	0.18
68-1, 29-31	<i>N. Trumpeyi</i>	656.49	-3.01	0.35

Table 7 (continued).

Core, section, interval (cm)	Species	Depth (m)	$\delta^{18}\text{O}$ (PDB)	$\delta^{13}\text{C}$ (PDB)
105-647A-68-3, 74-76	<i>Oridorsalis</i>	659.94	-3.01	-0.60
68-3, 74-76	<i>N. Trumpeyi</i>	659.94	-2.78	0.25
68-3, 74-77	<i>Cibicidoides</i>	659.94	-3.26	0.29
30-1, 51-53	Bulk	279.91	-0.32	0.87
36-4, 42-44	Bulk	342.12	-1.39	-4.32
36-4, 42-44	Bulk	342.12	-1.29	-3.78
38-6, 67-69	Bulk	364.57	-2.60	-6.23
43-4, 25-27	Bulk	409.55	-3.09	-2.54
46-5, 111-113	Bulk	440.91	-3.40	-1.69
48-1, 7-9	Bulk	453.27	-3.57	-3.95
50-4, 32-34	Bulk	477.32	-2.11	-2.06
51-4, 68-70	Bulk	487.28	-1.38	-5.68
51-4, 68-70	Bulk	487.28	-1.99	-6.03
51-6, 83-83	Bulk	490.43	-1.45	-0.43
52-2, 10-12	Bulk	493.40	-2.89	-0.16
53-4, 79-81	Bulk	506.45	-1.47	-7.04

values suggest somewhat deeper burial diagenesis, as discussed below.

**Bulk Sample Analyses**

Stable isotope analyses were also conducted on a limited number of bulk samples. The oxygen isotopic composition of these samples shows considerable variation with depth, similar to that observed in the benthic-foraminiferal isotope record. The heaviest measured values occur in the lower Oligocene part of the sequence, where a single sample at 279.91 mbsf yielded a  $\delta^{18}\text{O}$  value of  $-0.32\text{‰}$ . The gradual depletion in bulk-sample oxygen isotope composition occurs from 300 to 400 mbsf, with a trend similar to that recorded by the benthic foraminifers. Below 400 mbsf, bulk-sample  $\delta^{18}\text{O}$  values vary between  $-3.57$  and  $-1.38\text{‰}$ , with the lighter values generally corresponding to the lighter benthic foraminiferal values. The correspondence between bulk-sample and benthic foraminifers records suggest that burial diagenesis affected the isotopic composition of the benthics, as well as the bulk carbonate (mainly fine fraction).

A simple model can be constructed that constrains the timing and conditions under which burial diagenesis here may have occurred. Using a slightly modified equation of Killingley (1983) and assuming a closed system, a set of simple equations can be derived to calculate the "final" composition of the recrystallized carbonate ( $\delta^{18}\text{O}_{r-f}$ ), as well as the overall effect on the bulk-carbonate composition ( $\delta^{18}\text{O}_{b-f}$ ), if the initial composition of the carbonate is known or can be estimated.

$$\delta^{18}\text{O}_{r-f} = M_C R [\delta^{18}\text{O}_{b-i} + 10^3(1 - \alpha T)] + M_{iw} \delta^{18}\text{O}_{iw} \quad (1)$$

$$(M_{iw} + M_C) \alpha T.$$

$$\delta^{18}\text{O}_{b-f} = R \delta^{18}\text{O}_{r-f} + (1 - R) \delta^{18}\text{O}_{b-i} \quad (2)$$

In these equations,  $\delta^{18}\text{O}_{b-i}$  is the initial composition of the bulk carbonate and  $R$  is the percentage of the bulk carbonate that undergoes dissolution and/or recrystallization. The initial composition of the interstitial waters,  $\delta^{18}\text{O}_{iw}$  is derived from analyses of Zachos and Cederberg (Fig. 12A and this volume), which show a  $-0.88\text{‰}$  (SMOW)/100 m gradient at this site. The initial bottom-water oxygen isotopic composition is assumed to be  $0\text{‰}$  (SMOW). The number of moles of carbonate,  $M_C$ , and interstitial water,  $M_{iw}$  at the site of recrystallization, were determined using wet bulk density (WBD) (Srivastava, Arthur, et al., 1987) and percent carbonate (%  $\text{CaCO}_3$ ) data (Fig. 1; Table 1) in the following equations:

tervals of high Fe, Mn,  $P_2O_5$ , and associated elements, which are related to authigenic carbonate and apatite precipitates. The origin of these and other geochemical characteristics of the Eocene-Oligocene sequence is discussed below.

The diagenetic precipitation of Fe and Mn-carbonate minerals in Tertiary hemipelagic sediments is not that unusual. Disseminated and nodular siderite has been described from the late Paleogene and Neogene from a number of DSDP sites in the western North Atlantic (Sites 102, 104—Lancelot et al., 1972; Site 533—Matsumoto, 1983; Site 603—von Rad and Botz, 1986) and Pacific (Middle America Trench: Wada et al., 1982; Japan Trench: Matsumoto and Matsuhisa, 1986). These occurrences are in hemipelagic sequences characterized by high rates of deposition and preservation of sufficient organic matter to promote total consumption of dissolved sulfate by bacterial sulfate reduction, followed by strong methanogenesis (e.g., von Rad and Botz, 1986; Matsumoto, 1983; Claypool and Kaplan, 1984). Dolomite occurs in many of the same sediments that contain siderite. Matsumoto (1983) argued that dolomite precipitation occurs at relatively shallow depths in the Blake-Bahama Outer Ridge (Site 533) during late stages of sulfate reduction and early methanogenesis, followed by authigenic siderite at greater depth within the sediment. Similar results were obtained for Japan Trench sediments using oxygen and carbon isotope constraints (e.g., Irwin et al., 1977; Okada, 1980; Wada and Okada, 1983; Matsumoto and Matsuhisa, 1986).

The growth of Fe and Mn authigenic phases clearly requires the elevated alkalinity,  $CO_3^{2-}$  and  $TCO_2$  concentrations that accompany extensive degradation of organic matter, as well as a source of soluble Fe and Mn that are released under low redox conditions. Siderite precipitation also implies available Fe in excess of that necessary to form pyrite from the dissolved sulfide that results from bacterial sulfate reduction.

#### Timing and Geochemical Conditions of Precipitation

The carbon and oxygen isotopic compositions of discrete carbonate nodules provide constraints on the timing of precipitation and origin of the authigenic Fe-Mn carbonates (e.g., Irwin et al., 1977; Gautier, 1985). Carbon isotopic compositions of the homogenized nodules (no attempt was made to examine possible zonation of nodules in this study) range between  $-2$  and  $-6\text{‰}$  (PDB). These values indicate that carbonate ion was drawn from a somewhat  $^{13}C$ -depleted pore-water carbon reservoir that resulted from oxidation of organic matter. Pore-water dissolved sulfate concentrations (Zachos and Cederberg, this volume) reach a minimum at 500 mbsf but do not decrease below about 13 mmol/L. Thus, sufficient reactive organic matter may have been available to promote consumption of initial dissolved oxygen and partial bacterial sulfate reduction, but methanogenesis may never have occurred. This was confirmed when monitoring of head-space gas during drilling at Site 647 detected no methane (Srivastava, Arthur, et al., 1987). Present sedimentary organic carbon contents are generally low, ranging from 0.2 to 0.5 wt% (Fig. 1). Because there was insufficient pore water with which to determine total dissolved inorganic carbon (TDC) or  $\delta^{13}C_{TDC}$ , we must estimate the  $\delta^{13}C_{TDC}$  on the basis of a  $\Delta SO_4^{2-}$  of about 15 mmol/L, assuming a  $\Delta SO_4^{2-} : HCO_3^-$  ratio of 1:2 (TDC increases in proportion to the sulfate decrease) during sulfate reduction and a  $-22\text{‰}$   $\delta^{13}C$  value for the largely marine organic matter undergoing oxidation. The calculated minimum pore-water  $\delta^{13}C_{TDC}$  value is about  $-20\text{‰}$ . Therefore, it is likely that the authigenic Fe-Mn carbonates precipitated during early diagenesis, before the main phase of bacterial sulfate reduction, or that the Fe-Mn carbonates are a partial replacement of preexisting calcium carbonate having initially heavier  $\delta^{13}C$ . The  $\delta^{18}O$  values of the nodular carbonates have a range of  $-1.30$  to  $-3.50\text{‰}$  (PDB) (Table 7). Using these

data to estimate temperatures of formation is difficult because oxygen-isotopic fractionation factors between water and siderite and phosphoric acid and siderite have only recently been experimentally determined (Carothers et al., 1988). The isotope fractionation effects of bonding of different metals with carbonate also have been estimated theoretically (Tarutani et al., 1969), and Sharma and Clayton (1965) reported the fractionation factor for rhodochrosites. Siderite should be about 0.9‰ to 1.5‰ heavier than coexisting calcite; whereas, rhodochrosite should be similar in composition to coprecipitated calcite. Using an assumed  $\delta^{18}O$  of Eocene seawater of  $-1.2\text{‰}$  (SMOW; pre-glacial), the estimated temperature range for siderite or rhodochrosite precipitation would be  $28^\circ$  to  $30^\circ C$ . Estimated bottom-water temperatures for the Atlantic Ocean during the mid-to-late Eocene range from  $8^\circ$  to  $12^\circ C$  (e.g., Shackleton, 1986; Miller et al., 1985), so that the  $\delta^{18}O$  data from the nodules suggest precipitation following some burial. Pore water  $\delta^{18}O$  at Site 647 (below about 300 mbsf) is presently about  $-3\text{‰}$  (SMOW; Zachos and Cederberg, this volume), which at *in-situ* temperatures of about  $35^\circ C$ , would produce siderite with a  $\delta^{18}O$  of about  $-5$  to  $-6\text{‰}$  (PDB). Therefore, the authigenic carbonate nodules formed at shallow depths of burial, perhaps no more than 100 to 200 m. Separation of pure mineral phases for isotopic studies was not possible, and one must keep in mind that we analyzed only mixtures, which precludes a more detailed interpretation of the  $\delta^{18}O$  values at this time.

Whereas previous research suggests an association of Fe- and Mn-carbonates with methanogenesis, our data from Site 647 indicate that such geochemical conditions are not a prerequisite (see also Suess, 1979). However, there is little doubt that such mineralization is more extensive in methane-associated settings, which may be true for anoxic dolomites as well (e.g., Kelts and McKenzie, 1982).

One can see by inspection that the highest Fe/Al ratios (Fig. 13) occur in the intervals of documented increase in the relative abundance of concretions or nodules and that some, but not all, of the high Fe/Al ratios correspond to intervals of higher Fe/Mn as well. We would expect redox separation of Fe from Mn, as it has been described from many modern environments (e.g., Froelich et al., 1979; Li, 1982). Because of the effect of dilution of Al by higher carbonate contents and because both Fe and Mn are incorporated in the carbonate phases in varying amounts, we have also plotted the moving correlation coefficient for the relationship between Fe/Al and Fe/Mn ratios in Figure 13. The correlation coefficients indicate variation mainly between intervals of strong negative ( $r = -0.65$ ) and relatively, strong positive ( $r = 0.60$ ) correlation. Over much of the sequence (260-415 mbsf; 465-485 mbsf) variations in Fe and Mn concentrations may be positively correlated, even though the Fe/Mn ratio varies considerably. A few intervals of generally positive Fe/Al—Fe/Mn correlation (415-465 mbsf and  $>500$  mbsf) are mainly characterized by lower concentrations of Fe and Mn overall. These are most likely the "source" intervals from which the necessary "excess" Fe, and particularly excess Mn, migrated for precipitation as authigenic phases. Coarse-grained, initially more carbonate-rich beds may have catalyzed precipitation. We were unable to confirm this by examining the cores, but the need for some sort of coarser-grained nucleation site was postulated by Pederson and Price (1982) for more recent nonmethane-associated manganese-carbonates of the Panama Basin. Bohrmann and Thiede (this volume) examined Fe-Mn carbonates from deeper in the sequence in Hole 647A (Cores 105-647A-62 through -71) and found that they commonly occur as precompaction burrow-filling cements and that Mn is more important than Fe in cation substitution into the authigenic carbonate phases. Iron concentrations are higher on average in the lower part of lithologic Unit III that we analyzed, and in nodu-

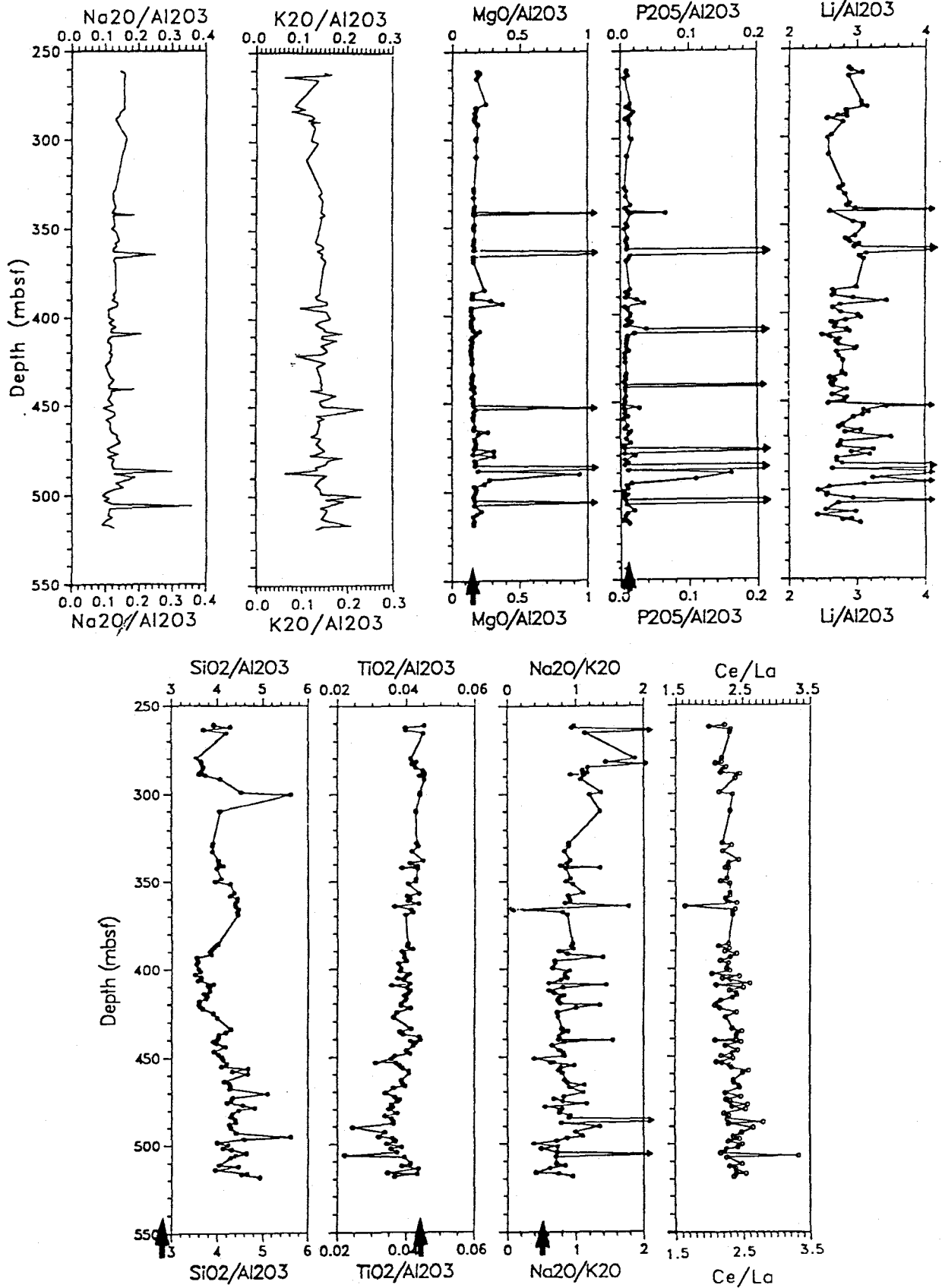


Figure 15. A.  $\text{SiO}_2/\text{Al}_2\text{O}_3$ ,  $\text{TiO}_2/\text{Al}_2\text{O}_3$ ,  $\text{Na}_2\text{O}/\text{K}_2\text{O}$ , and  $\text{Ce}/\text{La}$  ratios plotted downhole for lithologic Unit III C of Hole 647; arrows on bottom axis denote average Atlantic red clay (V26-157) values. B.  $\text{Na}_2\text{O}/\text{Al}_2\text{O}_3$ ,  $\text{K}_2\text{O}/\text{Al}_2\text{O}_3$ ,  $\text{MgO}/\text{Al}_2\text{O}_3$ ,  $\text{P}_2\text{O}_5/\text{Al}_2\text{O}_3$ , and  $\text{Li}/\text{Al}_2\text{O}_3$  values for lithologic Unit III C of Hole 647A plotted downcore.

- Chester, R., and Aston, S. R., 1976. The geochemistry of deep-sea sediments. In Riley, J. P., and Chester, R. (Eds.), *Chemical Oceanography*: New York (Academic Press), 6:281-390.
- Claypool, G. E., and Kaplan, I. R., 1974. The origin and distribution of methane in marine sediments. In Kaplan, I. R. (Ed.), *Natural Gases in Marine Sediments*: New York (Plenum Press), 99-139.
- Collier, R., and Edmond, J., 1984. The trace element geochemistry of marine biogenic particulate matter. *Prog. Oceanogr.*, 13:113-199.
- Dean, W. E., and Pahrduhn, N. L., 1984. Inorganic geochemistry of sediments and rocks recovered from the southern Angola Basin and adjacent Walvis Ridge, Sites 530 and 532, Deep Sea Drilling Project Leg 75. In Hay, W. W., Sibuet, J.-C., et al., *Init. Repts. DSDP*, 75 (Pt. 2): Washington (U.S. Govt. Printing Office), 923-958.
- Friedman, I., and O'Neil, J. R., 1977. Compilation of stable isotope fractionation factors of geochemical interest. In Fleischer, M. (Ed.), *Data of Geochemistry*. U.S. Geol. Surv. Prof. Pap., 440KK.
- Froelich, P. N., Klinkhammer, G. P., Bender, M. L., Luedtke, N. A., Heath, G. R., Cullen, D., Dauphin, P., Hammond, D., Hartman, B., and Maynard, V., 1979. Early oxidation of organic matter in pelagic sediments of the eastern equatorial Atlantic: suboxic diagenesis. *Geochim. Cosmochim. Acta*, 43:1075-1090.
- Goldschmidt, V. M., 1958. *Geochemistry*: London (Oxford Univ. Press).
- Huffman, E. W. D., 1977. Performance of a new automatic carbon dioxide coulometer. *Microchem. J.*, 22:567-573.
- Irwin, H., Curtis, C. D., and Coleman, M., 1977. Isotopic evidence for source of diagenetic carbonates formed during burial of organic-rich sediments. *Nature*, 269:209-213.
- Keigwin, L., 1980. Paleooceanographic change in the Pacific at the Eocene/Oligocene boundary. *Nature*, 277:722-725.
- Keigwin, L., and Corliss, B., 1986. Stable isotopes in Eocene/Oligocene foraminifera. *Geol. Soc. Am. Bull.*, 163:197-236.
- Kelts, K., and McKenzie, J. A., 1982. Diagenetic dolomite formation in Quaternary anoxic diatomaceous muds of Deep Sea Drilling Project Leg 64, Gulf of California. In Curran, J., Moore, D. G., et al., *Init. Repts. DSDP*, 64 (Pt. 2): Washington (U.S. Govt. Printing Office), 553-570.
- Killingly, J., 1983. Effects of diagenetic recrystallization on  $^{18}\text{O}/^{16}\text{O}$  values of deep-sea sediments. *Nature*, 301:594-597.
- Klovan, J. E., and Miesch, A. T., 1976. Extended CABFAC QMODEL computer programs for Q-mode factor analysis of compositional data. *Comp. Geosci.*, 1:161-178.
- Lancelot, Y., Hathaway, J., and Hollister, C. D., 1972. Lithology of sediments from the western North Atlantic, Leg 11, Deep Sea Drilling Project. In Hollister, C. D., Ewing, J., et al., *Init. Repts. DSDP*, 11: Washington (U.S. Govt. Printing Office), 901-949.
- Li, Y.-H., 1982. Interelement relationship in abyssal Pacific ferromanganese nodules and associated pelagic sediments. *Geochim. Cosmochim. Acta.*, 46:1053-1060.
- McCorkle, D. C., 1987. Stable carbon isotopes in deep-sea pore waters: modern geochemistry and paleoceanographic implications [Ph.D. dissert.]. Univ. of Washington, Seattle.
- Miller, K. G., Curry, W. B., Ostermann, D. R., 1985. Late Paleogene (Eocene to Oligocene) benthic foraminiferal oceanography of the Goban Spur region. In de Graciansky, P. C., Poag, C. W., et al., *Init. Repts. DSDP*, 80: Washington (U.S. Govt., Printing Office), 1089-1106.
- Miller, K. G., Fairbanks, R. G., and Mountain, G. S., 1987. Tertiary oxygen isotope synthesis, sea-level history, and continental margin erosion. *Paleoceanography*, 1:1-19.
- Matsumoto, R., 1983. Mineralogy and geochemistry of carbonate diagenesis of the Pliocene and Pleistocene hemipelagic mud on the Blake Outer Ridge, Site 533, Leg 76. In Sheridan, R. E., Gradstein, F. M., et al., *Init. Repts. DSDP*, 76: Washington (U.S. Govt. Printing Office), 411-427.
- Matsumoto, R., and Matsuhisa, Y., 1986. Chemistry, carbon oxygen and isotope ratios, and origin of deep-sea carbonate at Sites 438, 439, and 584: inner slope of the Japan Trench. In Kagami, H., Kang, D. E., et al., *Init. Repts. DSDP*, 87: Washington (U.S. Govt. Printing Office), 669-678.
- Müller, P. S., and Suess, E., 1979. Productivity, sedimentation rate, and sedimentary organic carbon content in the oceans. *Deep-Sea Res.*, 26:1347-1362.
- Okada, H., 1980. Pebbles and carbonate nodules from Deep Sea Drilling Project Leg 56 cores. In Scientific Party, *Init. Repts. DSDP*, 56, 57(Pt. 2): Washington (U.S. Govt. Printing Office), 1089-1106.
- Pederson, T. F., and Price, N. B., 1982. The geochemistry of manganese carbonate in Panama Basin sediments. *Geochim. Cosmochim. Acta*, 46:59-68.
- Piper, D. Z., and Graef, P. A., 1974. Gold and rare-earth elements in sediments from the East Pacific Rise. *Mar. Geol.*, 17:287-297.
- Sayles, F. L., Ju, T. K., and Bowker, P. C., 1975. Chemistry of ferromanganese sediment of the Bauer Deep. *Geol. Soc. Am. Bull.*, 86: 1423-1431.
- Shackleton, N. J., 1986. Paleogene stable isotope events. *Palaeogeogr., Palaeoclimatol., Palaeocol.*, 57:91-102.
- Shackleton, N. J., and Kennett, J., 1975. Paleotemperature history of the Cenozoic and the initiation of Antarctic glaciation; oxygen and carbon isotope analysis in DSDP Sites 277, 279, 281. In Kennett, J. P., Houtz, R. E., et al., *Init. Repts. DSDP*, 29: Washington (U.S. Govt. Printing Office), 743-755.
- Sharma, T., and Clayton, R. N., 1965. Measurement of  $^{18}\text{O}/^{16}\text{O}$  ratios of total oxygen from carbonates. *Geochim. Cosmochim. Acta*, 29: 1347-1354.
- Suess, E., 1979. Mineral phases in anoxic sediments by microbial decomposition of organic matter. *Geochim. Cosmochim. Acta*, 43: 339-352.
- Tarutani, T., Clayton, R. N., and Mayeda, T. K., 1969. The effect of polymorphism and magnesium substitution on oxygen isotope fractionation between calcium carbonates and water. *Geochim. Cosmochim. Acta*, 33:987-996.
- von Rad, V., and Boiz, R., 1986. Authigenic Fe-Mn carbonates in Cretaceous and Tertiary sediments of the continental rise off eastern North America, DSDP Site 603. In van Hinte, J., Wise, S., et al., *Init. Repts. DSDP*, 93: Washington (U.S. Govt. Printing Office), 1061-1078.
- Wada, H., Niitsuma, N., Nagasawa, K., and Okada, H., 1982. Deep-sea carbonate nodules from the Middle America Trench area off Mexico, Deep Sea Drilling Project Leg 66. In Watkins, J. S., Moore, J. C., et al., *Init. Repts. DSDP*, 66: Washington (U.S. Govt. Printing Office), 453-474.
- Wada, H., and Okada, H., 1983. Nature and origin of deep-sea carbonate nodules collected from the Japan Trench. In Watkins, J. S., and Drake, C. L. (Eds.), *Studies in Continental Margin Geology*. AAPG Mem, 34:661-672.
- Wedepohl, K. H., 1971. *Geochemistry*: New York (Holt, Rinehart, and Winston).

Date of initial receipt: 5 April 1988

Date of acceptance: 3 February 1989

Ms 105B-157